Accepted Manuscript

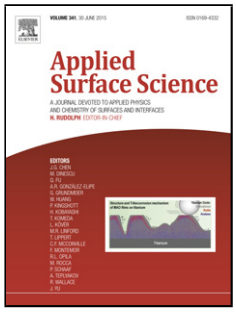

Title: Mg_2Sn heterostructures on Si(111) substrate

Authors: L. Dózsa, N.G. Galkin, B. Pécz, Z. Osváth, Zs. Zolnai, A. Németh, K.N. Galkin, I.M. Chernev, S.A. Dotsenko

PII: S0169-4332(17)30337-9
DOI: http://dx.doi.org/doi:10.1016/j.apsusc.2017.01.299
Reference: APSUSC 35094

To appear in: *APSUSC*

Received date: 8-8-2016
Revised date: 18-11-2016
Accepted date: 30-1-2017

Please cite this article as: L.Dózsa, N.G.Galkin, B.Pécz, Z.Osváth, Zs.Zolnai, A.Németh, K.N.Galkin, I.M.Chernev, S.A.Dotsenko, Mg2Sn heterostructures on Si(111) substrate, Applied Surface Science http://dx.doi.org/10.1016/j.apsusc.2017.01.299

Mg_2Sn heterostructures on Si(111) substrate

L. Dózsa[1], N.G. Galkin[2,3], B. Pécz[1], Z. Osváth[1], Zs. Zolnai[1],A. Németh[4], K. N. Galkin[2], I.M. Chernev[2] and S.A. Dotsenko[2,3]

[1] Institute of Technical Physics and Materials Science, Centre for Energy Research, Hungarian Academy of Sciences, 1525 Budapest Pf, 49, Hungary

[2]Institute of Automation and Control Processes of FEB RAS, 5 Radio St., Vladivostok 690041, Russia

[3] Far Eastern Federal University, 8 Sukhanova St., Vladivostok, 690950, Russia

[4] Wigner Research Centre for Physics, Institute for Particle and Nuclear Physics, 1525 Budapest, P.O.B. 49, Hungary

*e-mail: corresponding_author dozsa@mfa.kfki.hu

Highlights

Investigations show that the nanostructures have significant changes during a regular experimental investigations, and time order of the investigations has a dominant effect on the results.

It is especially true for transmittance electron microscopy, where the investigated layers have

Abstract. Thin un-doped and Al doped polycrystalline Mg-stannide films consisting mainly of Mg_2Sn semiconductor phase have been grown by deposition of Sn-Mg multilayers on Si(111) p-type wafers at room temperature and annealing at 150 ^oC. Rutherford backscattering measurement spectroscopy (RBS) were used to determine the amount of Mg and Sn in the structures. Raman spectroscopy has shown the layers contain Mg_2Sn phase. Cross sectional transmission electron microscopy (XTEM) measurements have identified Mg_2Sn nanocrystallites in hexagonal and cubic phases without epitaxial orientation with respect to the Si(111) substrate. Significant oxygen concentration was found in the layer both by RBS and TEM. The electrical measurements have shown laterally homogeneous conductivity in the grown layer. The undoped Mg_2Sn layers show increasing resistivity with increasing temperature indicating the scattering process dominates the resistance of the layers, i.e. large concentration of point defects was generated in the layer during the growth process. The Al doped layer shows increase of the resistance at low temperature caused by freeze out of free carriers in the Al doped Mg_2Sn layer. The measurements indicate the necessity of protective layer grown over the Mg_2Sn layers, and a short time delay between sample preparation and cross sectional TEM analysis, since the unprotected layer is degraded by the interaction with the ambient.

Keywords: MgSn nanocrystals grown in silicon;
Thermoelectric materials
stability of nanostructures grown in silicon

1. Introduction

Magnesium silicides and -stannides (Mg_2X (X=Si, Sn) [1-5], and their ternary alloys attracted attention as ecologically clean semiconductors, which consist of abundantly available, relatively cheap non-toxic materials. In the first time these silicides, stannides and their alloys [6-8] drew the attention as candidates of efficient thermoelectric materials due to their large Seebeck coefficient (α), high electrical conductivity (σ), and low thermal conductivity (k). It is known that Mg_2X compounds possess higher value of the power factor and thermoelectric figure of merit than GeSi alloys and β-$FeSi_2$ [9], so they are promising materials for production of high efficiency thermoelectric convertors.

The preparation of the ternary alloy of these compounds $Mg_2Si_{1-x}Sn_x$ is a perspective from the point of view of increasing electrical conductivity and decreasing thermal conductivity due to complex phonon structure of the alloy [10,11]. The detailed study of Mg_2Si and Mg_2Sn compounds and their quasi-binary alloys [8] have shown that Mg_2Si - Mg_2Sn system is preferable for thermoelectrical applications due to combination of electrical properties and band structure. Since Si and Sn atoms posess large difference in atomic mass, the $Mg_2Si_{1-x}Sn_x$ solid alloys exhibit small lattice thermal conductivity. Therefore, this system is preferable for the production ot thermoelectric converters compared with Mg_2Si - Mg_2Ge and Mg_2Ge – Mg_2Sn systems. In addition the Mg_2Si-Mg_2Sn system has a peculiarity in its band structure connected with the splitting of conduction band in the direction of *X* valley according to theoretical calculations [12]. The second conductivity band is separated from the first one by an energy gap from 0.2 eV to 0.6 eV depending on the type of chemical compound. In the $Mg_2Si_{1-x}Sn_x$ binary compound this gap value can decrease to near zero in a range of "x" value that provide an increase of density of states and result in increase of the carrier concentration and thermoelectric motive force without additional doping of the compound compound. Investigations of bulk $Mg_2Si_{0.4}Sn_{0.6}$ and $Mg_2Si_{0.6}Sn_{0.4}$ have shown [13,14] that the value of the dimensionless thermoelectric figure of merit *ZT* reaches 1.4 – 1.6 values at temperatures of 600 – 700 K, showing a prospects of these materials for the production of effective and ecologically clean thermoelectric converters.

The doping of Mg_2Sn and Mg_2Si compounds is a serious problem for using them as thermoelectric materials. It is known that Mg_2Si monocrystals grown from melt with stoichiometric Mg/Si relation without additional doping are n-type semiconductor [15]. Non-stoichiometry influences the conductivity type of these compounds. In Mg_2Si this effect is not

exactly determined, but for Mg_2Ge it is known that the excess of Ge atoms results in the change of the conductivity type from p- to n-type. Investigations of Mg_2Sn compounds have shown that doping by Ag, Ga and Cu results to p-type conductivity, but doping by Sb, Al and B results in n-type conductivity [16-22].

In this work, as a first step to prepare $Mg_2Sn_xSi_{1-x}$ compound semicomndoctor thermoconverter integrated to silicon, Mg_2Sn was grown by solid phase epitaxy on p-type silicon substrate (Si(111)7x7) and effects of doping by Al was investigated by optical measurements, Rutherford backscattering, Raman spectroscopy, transmission electron microscopy, by current-voltage (I-V), capacitance voltage (C-V) and deep level transient spectroscopy (DLTS) characterization of Schottky junction prepared on the grown films were used to investigate the properties of the layers.

2. Experiment

Growth experiments were carried out in ultra-high vacuum (UHV) VARIAN chamber with base pressure of $2x10^{-10}$ Torr equipped with Auger and electron energy loss spectrometer (AES-EELS). Sublimation sources of Sn and Mg, and quartz sensors for measurement of the deposited film thickness. 45 Ω·cm p-type boron doped Si(111) wafer fragments were used as substrate. The details of Mg_2Sn solid phase epitaxy (SPE) growth was described in [23]. The Mg_2Sn film was formed from 8 Sn-Mg bilayers (Sn layer is the first one), deposited at room temperature on atomically clean silicon surface (Si(111)7x7) and annealed in a single step at 150 ^oC after finishing the eight deposition cycles. The doping was performed by deposition of Al between the Sn and Mg layers in each cycle and activating the dopant during the 10 minute annealing at 150 ^oC after the deposition of the eighth Sn-Al-Mg layers. The Sn, Mg, and Al deposition rates (0.3 – 1.5 nm/min) were measured by quartz microbalance. The deposition rate has not been precisely controlled during deposition, and the deposited elements may evaporate from the surface, that demands the control of the thicknesses by cross-section high-resolution transmission electron microscopy (HR XTEM).

The morphology of the samples was investigated by atomic force microscopy (AFM) in contact and tapping modes. Raman spectra were registered at room temperature on "WITec alpha 300 RSA+" confocal Raman microscope (HAS, Hungary) with 488 nm wavelength laser excitation. The RBS measurements were carried out using 1 MeV He^+ ion beam and measuring the reflected beam at 165º with an ORTEC type surface barrier detector installed in the scattering chamber connected to a 5 MV Van de Graaff accelerator (Wigner Research Center for Physics, HAS). A Philips CM 20 TEM at 200 keV was used to measure planar and

cross-sectional specimens, and a JEOL 3010 HR TEM equipped with an energy filtering attachment (EFTEM) was also applied. The electrical characteristics and point defects in the grown structures were investigated by current–voltage (I-V), capacitance-voltage (C-V), and deep level transient spectroscopy (DLTS) measurements in Schottky junctions prepared by deposition of rectangular 400x400 μm Au dots over the grown layers.

3. Results

3.1 Sample preparation and in situ experiments

The growth of the magnesium stannide (Mg_2Sn) layers on the atomically clean Si(111) surface was started by room temperature deposition of the Sn/Al/Mg layers given in Table I. The deposition of the layers was repeated in 8 cycles.

Investigations of the electronic structure of the grown Mg_2Sn films by *in situ* AES have shown that the as grown films consist mainly of Mg_2Sn phase and a small quantity of Mg_2Si phase [23]. AFM has measured root-mean square roughness of 2.3 – 3.5 nm that indicates a continuous film formation. Far infrared (FIR) properties of grown Mg_2Sn films have also proved the formation of Mg stannide with small quantity of Mg silicide [23]. The results presented in [23] were measured short after removing the samples from the growth chamber, while the results presented in this work characterize samples about 6 -12 month after sample preparations.

3.2 Rutherford backscattering spectroscopy

1 MeV He^+ RBS spectra have been measured a few months after the samples were removed from the vacuum chamber, so possible oxidation in the ambient must be considered in their analysis. Fig.1a shows the 1 MeV He+ RBS spectra of the undoped and Al doped samples measured at 7° sample tilt, while Fig.1b shows the spectra measured in the undoped Mg_2Sn sample at 7° and 60° tilt angle with and the spectrum simulation line fits. RBS spectrum evaluation and fitting has been performed with the RBX simulation program [24]. The structure for each sample was assumed to be a 2-layer or 3-layer system with different Sn, Mg, and O contents. Oxygen was detected in the samples and considered in the simulations. Parameters used in best fits of the simulated RBS spectra of the Al doped samples are listed in Tables II. The effective thicknesses in Table II are given in units of atom/cm^2. In RBS the He^+ beam spot size is about ,0.5 mm x 0.5 mm so the compositions and thicknesses evaluated from RBS are averages in this area. These compositions were refined in depth by assuming the two or three-layer models. The smeared character of the Sn, Mg, Si,

and O spectra requires the refinement of the model structure as a single layer model is not appropriate to reconstruct the measured datasets. To achieve increased accuracy of the evaluation, RBS measurements were carried out at two different sample tilt angles (7^o and 60^o), and the spectra were simultaneously fitted by the RBX program using the same model structure for both tilt angles (see Fig. 1(b)). Indeed, the Sn, Mg, Si, and O spectra are cross-linked through the sublayer compositions and we believe that our evaluation gives a composition and total amount of the components close to the real values. Further details of the RBS analysis of thin layer structures can be found in our previous work on the characterization of BeMgZnO quaternary alloys [25].

Considering the slight shift of the Si edge with respect to pure Si we considered that the top layer of the samples does not contain silicon.However, significant amount of oxygen appears which we assume was incorporated after removal of the samples from the vacuum chamber. Note, RBS provides information on the total number of atoms per unit area in the layer analysed but does not give information on the chemical state of the different constituents. The oxygen signal sits on a large background given by the Si spectrum. Also, the intensity of the O peak is small due to the low scattering cross-section for O. Therefore, the accuracy of the analysis for O is smaller than for the heavier elements, e.g., Sn and Mg. Nevertheless, the presence of O is clearly seen, especially in the spectra recorded at 60^o sample tilt angle (see Fig. 1b). By varying the oxygen content in the sublayers during the evaluation, the height of the Mg and Sn spectra can be reconstructed.The composition of the top layer determined by RBS is equivalent to 70% MgO, 7 % Mg_2Sn, and 23 % SnO_2 composition. It shows that the top 12 nm layer was almost completely oxidized during the storage in the ambient for about one year. In the second layer fitted by RBS a considerable amount of Si (54 %) appears, while the amount of Sn is low (6%). The amount of Mg (40 %) is low for the nominal composition; the Mg_2Sn seems to be embedded in Si. The composition measured by RBS shows that the layer composition is appropriate for 10 % Mg_2Sn, 23 % Mg_2Si, and 67 % Si phase in this layer. The thickness of this layer is about 17-18 nm. The total Sn (3 nm) and Mg (11.9 nm) contents are appropriate for only about 1 cycle of deposition. These thickness values were calculated assuming atomic densities for Sn and Mg of $N = 3.7\times10^{22}/cm^3$, and $N = 4.3\times10^{22}/cm^3$, respectively.

The composition in the 3 layers fitted by RBS in the undoped sample is given in Table III. The surface layer is dominated by oxygen also in this sample.

Interpretation of the layer composition as a mixture of MgO (68 %), Mg_2Sn (11%), and SnO_2 (5%) phases shows that most of the top layer is oxidized also in the undoped sample. The thickness of this layer is about 15-16 nm in the area measured by RBS. Below the oxygen rich layer a Sn rich layer was found. This layer is dominated by Mg and Sn (about Mg_3Sn composition). The thickness of this layer is about 6 nm. The Si content fitted by RBS is significant in the 3rd layer, the Sn content is only about 8 %. The Mg (50 %) and Si (42 %) dominate this layer. The layer composition can be explained by Mg_2Sn (16 %), Mg_2Si (34%) and Si (50 %) phase composition. The total thickness of this layer measured by RBS is about 15 nm. The total amount of Sn (5.4 nm) and Mg (20 nm) in the undoped Mg_2Sn sample is appropriate for about 2 deposition cycles, using the atomic densities given above.

3.2 Raman measurements

The average Raman spectra of the Mg_2Sn samples are shown in Fig.2 by red line and dots and green line and triangles, respectively**.** The major peak at 220 cm^{-1} corresponds to Raman peak for bulk Mg_2Sn (222-224 cm^{-1}) [26,27], the second one at 252 cm^{-1} correlates with position of Raman peak (258 cm^{-1}) of bulk Mg_2Si [27]. It shows the formation of Mg silicide is not excluded during the growth of Mg stannide film on Si substrate due to intermixing of deposited Sn atoms and Si atoms of the substrate during the solid phase reaction. In the Al-doped sample the Raman peak (520 cm^{-1}) intensity of crystalline Si is comparable to Raman line intensities of Mg_2Sn (222-224 cm^{-1}) and Mg_2Si (252 cm^{-1}), while in the undoped sample this silicon line is much smaller. It indicates that the silicon is not fully covered by the Al-doped Mg_2Sn film. It correlates with the high roughness measured by AFM in these samples [23]. Raman maps recorded in the 200-235 cm^{-1} and 240-270 cm^{-1} regions have shown anti-correlation (Fig. 3 a,b) that correspond to appearance of two different phases: Mg_2Sn (peak at 220 cm^{-1}) and Mg_2Si (peak at 252 cm^{-1}) on the surface. The quantity of Mg_2Si is higher in the Al-doped sample due to higher intermixing of Si with Mg during the annealing. The key parameter in determination of the composition of the layer seems to be the amount of oxygen in the layer, which may react with Si, Mg, Al, and Sn atoms, and may change the composition during a storage in the ambient for about one year.

The map of the ratio of the Mg_2Sn and Mg_2Si peak intensity in the Raman spectra are shown in Fig.4a. The ratio varies from 0 to about 3 on the surface, i.e. in some regions mostly Mg_2Sn and in some other regions mostly Mg_2Si phase appears. The Si related peak at about 500 cm^{-1} is shown in Fig.4b. It is remarkable that the intensity of the Si peak is comparable to the Mg_2Sn line intensity, i.e. the silicon is not covered continuously by Mg_2Sn or Mg_2Si layer

in the Al doped sample. It suggests that in the Al doped samples some area is covered by some oxide which is transparent to the light used in Raman measurement.

3.3 *Transmission electron microscopy*

The HR XTEM image of the undoped sample measured 1 year after removing the samples from the vacuum chamber and about 1 month after thinning the samples for XTEM analysis and its fast Fourier transformation are shown in Fig. 5. Analysis of images by FFT has shown six reflections and three of them correspond to silicon planes (111), (220) and (311) (insert in Fig. 5). A few additional reflections in the local FFT were calculated in two areas. The first rectangular area is indicated by number '1' in Fig. 5. In this area the FFT image corresponds to the distances between the (311) planes of cubic magnesium stannide (cub-Mg_2Sn [12]), which proves the formation of cub-Mg_2Sn in the film. The second group (rectangle indicated by '2' in Fig. 5) contains areas with well-defined structures in the form of nanocrystallites (NCs). FFT pattern from these areas gives interplanar distances corresponding to hexagonal magnesium stannide: hex-Mg_2Sn(303) and hex-Mg_2Sn(311) [28]. The cub-Mg_2Sn NCs did not show preferential growth direction, the film is polycrystalline. If we compare the FFT image from hex-Mg_2Sn NCs and Si, it shows that this stannide is also polycrystalline. Apparently, amorphous Sn layer deposited onto the Si substrate prevents the nanocrystals to select the preferred growth direction. The XTEM image of the undoped Mg_2Sn samples is shown in Fig.6. It is apparent that the layer is not homogeneous, different size and shape particles can be seen. The layer thickness measured by TEM is in agreement with the results of RBS fit. The Mg, Sn, Si and O elementary maps of the same region are shown in Fig.7(a,b,c,d), respectively. It is apparent that in XTEM oxygen is seen in the whole layer in contrast to the model fit by RBS data, which fails to measure O in larger depth, since the O backscattering edge is below that of the Si. However, TEM investigation was carried out several months after RBS measurements, and sample preparation for TEM requires thinning of the samples, so it facilitates further oxidation of the layers. An elemental map analysis by EFTEM has confirmed that Mg, Sn, Si and O atoms are non-homogeneously distributed in the layers with a thickness of 35-50 nm as it is shown in Fig. 7 (a,b,c,d), respectively. It is apparent that the Mg and O maps are nearly identical, i.e. most of the Mg is in MgO composition, as it was indicated by RBS data. The silicon content in the top 30 nm of the MgO-Mg_2Sn layer is negligible. The thicknesses measured by TEM agree with the thicknesses measured and calculated by RBS model (30-40 nm), but they are still only about 60 % of the nominal values calculated from deposited amounts given in Tables I and II. Since

the amount of the Mg_2Sn is smaller than expected, this deficit can be caused by diffusion of these elements to the silicon bulk, by evaporation of Mg after deposition, and by errors in the Mg and Sn deposition rate determination. The XTEM measurements of the samples were repeated in 2015, about two years after the sample preparation, and about 1 year after the TEM sample preparation and first TEM measurements. The repeated HRTEM measurement shown in Fig. 8 proves that in the samples thinned for TEM measurements the composition and the previously detected Mg_2Sn phases are not visible, the composition and the structure of the grown layer drastically changes. The elemental maps of Sn, O, Si, C in the area shown in Fig.8 XTEM image are shown in Fig. 9 (a,b,c,d), respectively. The elementary maps show that Mg disappears, Sn and O are redistributed, Si moves into the top layer, and also carbon appears in the top layer instead of Mg. Future TEM measurements have to be carried out short after sample preparation, and short time after TEM sample preparation (thinning), since the components of the layer interact with the ambient, mostly with oxygen. AFM measurement measured in the Mg_2Sn sample stored in the ambient (not thinned for TEM investigation) were repeated in 2015. The height image of the undoped sample in of a 10x10 μm area is shown in Fig.10. The image was measured in the uncovered area of the wafer fragments used for electrical characterization. The structure has basically changed; it proves that the layer structure and composition significantly were also changed in the samples not thinned for XTEM measurement. Even the loss of Mg and Sn can be explained by the changes of the structure, so it is necessary in the future to grow a protective layer over the stannide/silicide film for further studies of these materials.

3.4 Electrical characteristics

The electrical characteristics were measured in 400x400 μm Schottky junctions prepared by deposition of 300 nm thick Au on the top of the prepared layer. The Schottky junctions were prepared short after Rutherford scattering and Raman experiment, about 6 month after growth of the layers. The measured current-voltage (I-V) characteristics of the doped and undoped layers at room temperature and at liquid N_2 temperature (77 K) are shown in Fig. 11 (a,b), respectively. The temperature dependence of capacitance of the Schottky junctions on Al doped and undoped Mg_2Sn samples are shown in Fig.12a. Fig.12b shows the temperature dependence of the current measured at +5V voltage in the Schottky junctions prepared over the undoped and Al doped Mg_2Sn samples. It is apparent that in the Al doped sample the deposited layer shows higher resistance and opposite temperature dependence. The undoped samples show decreasing current with increasing temperature, while in the doped samples the

current increases with increasing temperature, i.e. the thermal activation of the free carriers can be seen. The deposited layer electrical characteristics can be summarized saying that in the doped sample the Fermi level is pinned by point defects at about 120 meV from the valence band, and the current is not determined by the space charge, but by the resistivity of the grown layer, and DLTS spectra are dominated by the point defects present in the substrate. The point defects dominate the conductivity also in the undoped Mg_2Sn layer, however, in this case the free carriers in the layer do not show freeze out at low temperature, the current is not blocked by the grown layer at low temperature, i.e. the Fermi level in this layer is closer to the valence band of silicon. This fact is also supported by the results of the DLTS investigation. In all samples a defect similar to the defect found in the substrate was seen, which can be identified as some metallic (Ti -0,3 eV [29], Ni -0.32 eV, Mn -0.36 eV [30], C-C pair -0.37 eV [31],) contamination in the substrate.

4. Discussion

Investigations of the electronic structure of the grown Mg_2Sn films by *in situ* AES have shown that the as grown films consist mainly of Mg_2Sn phase and a small quantity of Mg_2Si phase [8]. Far infrared (FIR) properties of grown Mg_2Sn films have also proved the formation of Mg stannide with small quantity of Mg silicide. According to RBS the top layer of the samples does not contain silicon, but significant amount of oxygen appears which we assume was collected after removal of the samples from the vacuum chamber. The composition determined by RBS in the Al doped top layer is equivalent to 70% MgO, 7 % Mg_2Sn, and 23 % SnO_2 composition, in the undoped sample to MgO (68 %), Mg_2Sn (11%), and SnO_2 (5%) phases. It shows that most of the top layer is oxidized, especially in the Al doped sample.

In the Al doped sample the 18 nm layer below the top layer due to RBS is appropriate for 10 % Mg_2Sn, 23 % Mg_2Si, and 67 % Si phase content. In the undoped sample below the oxygen rich layer a 6 nm Sn rich layer was found by RBS. This layer is dominated by Mg and Sn (about Mg_3Sn composition). It suggests that some of the Mg is bound to O in this layer. The composition of this 6 nm layer may be 50 % Mg_2Sn and 50 % MgO. The Si content fitted by RBS also is significant in the undoped sample in the next layer (15 nm thick), the Sn content is only about 8 %. The layer composition can be explained by Mg_2Sn (16 %), Mg_2Si (34%) and Si (50 %) phase composition. If we assume that the dominant phase is a ternary silicide phase it has about $Mg_2Sn_{0.32}Si_{0.64}$ composition in the layer, however, TEM and Raman results suggests that the two silicide phases are grown separately. The total amount of Sn in the Al doped (3 nm) and undoped samples (5.4 nm) , and the amount of Mg in the Al doped

(11.9 nm) and in the undoped sample (20 nm) are appropriate for only about 1 and 2 cycles of deposition.

The Raman at 220 cm^{-1} corresponds to the bulk Mg_2Sn (222-224 cm^{-1}) [10,11], the peak at 252 cm^{-1} is near to the Raman peak of bulk Mg_2Si (258 cm^{-1}) [11]. In the Al-doped sample the Raman peak (520 cm^{-1}) of crystalline Si also appears in the spectrum, indicating that the silicon is not fully covered by the Al-doped film, some oxide areas covers the silicon wafer, as it is proved by the image of the silicon related Raman line. This fact correlates with the high roughness measured by AFM in the samples [8]. The ratio of the Mg_2Sn (peak at 220 cm^{-1}) and Mg_2Si peaks (240-270 cm^{-1}) in the Raman spectra shown in Fig.4c varies from 0 to about 3, i.e. in some regions mostly Mg_2Sn and in some other areas mostly Mg_2Si phase was found. The quantity of Mg_2Si is higher for the Al-doped sample, however, RBS has measured also higher Mg content in the undoped sample. The Al may cause intermixing of Si with Mg during annealing, however further experiments are needed to answer the question. The key parameter in determination of the composition seems to be the presence of O in the layer, which may react with Si, Mg, Al, and Sn atoms, and strongly influence the composition.

The Mg_2Sn NCs in XTEM did not show preferential growth direction, the film is polycrystalline. The amorphous Sn layer deposited onto the Si substrate prevents the nanocrystals to select the preferred growth direction.

The XTEM image of the undoped Mg_2Sn samples (Fig.6) shows the layer is not homogeneous, different size and shape particles can be distinguished. The layer thicknesses measured by TEM are in agreement with the results of RBS fit. The Mg, Sn, Si and O elementary maps show that oxygen is seen by XTEM in the whole layer, in contrast to the model fit by RBS data. RBS fails to measure O in larger depth, since the O backscattering edge is below that of the Si, however, TEM investigation was carried out several month after RBS measurements, and sample preparation for TEM requires thinning of the samples, so it facilitates further oxidation of the layers, so further experiments are needed to clearly answer the question.

An elemental map analysis by EFTEM after few month of TEM sample thinning for the measurement has confirmed that Mg, Sn and Si atoms are non-homogeneously distributed in the layers with a thickness of 35-50 nm as it is shown in Fig. 7. It is apparent that the Mg and O maps are nearly identical, i.e. most of the Mg is in MgO composition, as it was indicated by RBS. The silicon content measured by TEM in the top of the top 30 nm of the MgO-Mg_2Sn layer is negligible. The thicknesses measured by TEM agree with the thicknesses calculated

by RBS model (30-40 nm), but they are still only about 60 % of the nominal values calculated from deposited amounts given in Tables I and II. Since the amount of the Mg_2Sn is smaller than expected, this deficit can be caused diffusion of these elements to the silicon bulk and by errors in the Mg and Sn deposition rate determination. The TEM measurements of the samples were repeated in 2015, about two years after the sample preparation and about 1 year after the TEM sample thinning show that in the samples thinned for TEM measurements the composition and the previously detected Mg_2Sn phases are not visible, the Mg disappears, and C is incorporated in the layer. The results show that future TEM measurements have to be carried out short after sample preparation, and short after TEM sample thinning since the components of the layer interact with the ambient, mostly with oxygen and carbon. AFM images measured on the unprotected Mg_2Sn surface show that in the ambient the surface layer reacts with ambient, and loss of Mg and Sn may be also caused by diffusion of Mg from the layer, and interacting with oxygen, forming nanostructures shown in the AFM image.

The temperature dependence of current and capacitance of the Schottky junctions on Al doped and undoped Mg_2Sn samples show that resistance of the deposited layer dominates the electrical characteristics. The Al doped shows higher resistance, and the current increases with increasing temperature, i.e. the thermal activation of the free carriers can be seen. The deposited layer electrical characteristics can be summarized saying that in the Al doped sample the Fermi level at the interface is pinned by point defects at about 120 meV from the silicon valence band, and the current is not determined by the space charge, but by the resistivity of the grown layer. DLTS spectra are dominated by the point defects present in the substrate in both samples. The defect can be identified as some metallic (Ti -0,3 eV [13], Ni -0.32 eV, Mn -0.36 eV [13], C-C pair -0.37 eV [14],) contamination in the Si substrate. Electrical characterization repeated in the Schottky junctions after degradation of the surface show that a metal (in this case gold) is an appropriate layer to protect the grown layer from reaction with the ambient.

5. Conclusion

Mg_2Sn un-doped and Al doped layers were prepared by solid phase reaction on Si(111) substrate. It was shown that the grown films are nonhomogeneous in the thickness and composition, and mostly consist of separated Mg_2Sn and Mg_2Si phases. The formation of cub-Mg_2Sn and hex-Mg_2Sn has been observed for grown samples by analysis of HR TEM data. Oxides of the deposited metallic components also appear in the layer. The low amount of Mg and Sn found in the layer is partly explained by the calibration error of the vibrating quartz

sensor used in the experiments, and partly by the reduction of the amount of these elements with athe ambient during storage.The formation of Mg_2Sn and Mg_2Si has been observed in the samples within a year after their preparation, but these phases seem to be mostly destroyed by interaction with oxygen in the ambient, especially in the samples thinned for transmission electron microscopy investigation. Some repeated sample preparation including a protective layer prepared against oxidation and TEM analysis with short time delay after TEM sample thinning is necessary to determine the phases and structure of the freshly prepared Mg_2Sn layers. A general conclusion is that for evaluation of the thin layers (often used in production) by the classical measurement techniques (RBS, Raman, TEM etc.) have to be integrated with sample preparation vacuum chamber, since the few atomic layer structures are strongly affected by the interaction with the ambient.

Acknowledgments

This work is partially supported by RFBR grant No 13-02-00046_a and by the Hungarian National Scientific Research Fund (OTKA) Grant No. K108869. The authors thank Mr. A.V. Shevlyagin for participation in the sample growth.

References

[1] R.J. Labortz, D.R. Mason, D.F. O'kane, J. Electrochem. Soc. 110 (1963) 1274-1280;

[2] F. Fazquez, R.A. Forman, M. Cardona Phys. Rev. 176 (1968) 905-908;

[3] Y. Hayakawa, M. Arianandhan, Y. Saito, T. Koyama, a.o., Thin Solid Films 519 (2011) 8532;

[4] H. Ihoe-Mouko, C. Mercier, J. Tobola, G. Pont, H. Scherrer. J. Alloys & Comp. 509 (2011) 6503-6508;

[5] F. Yu, J-X. Sun, T-H. Chen Phys. B: Cond. Matt. 406 (2011) 1789-1794;

[6] Y. Noda, H. Kon, Y. Furukawa, N. Otsuka, I.A. Nishida, K. Masumoto. Mater. Trans. JIM 33 (1992) 845-856;

[7] J. Tani, H. Kido. Physica B 364 (2005) 218-223;

[8] V.K. Zaitsev, M.I. Fedorov, E.A. Gurieva, I.S. Eremin, P.P. Konstantinov, A.Yu. Samunin, a.o. Phys. Rev. B, **74**, 045207(1-8) (2006).

[9] C.B. Vining. *CRC Handbook of Thermoelectrics*. In: Rowe DM, editor. New York: CRC Press; 1995. p.277.

[10] M. Asaka, T. Iida, K. Nishio, Y. Takanashi. Thin Solid Films, **515**, 8237 (2007).

[11] H. Ihou-Mouko, C. Mercier, J. Tobola, G. Pont, H. Scherrer. J. Alloy and Compounds, **509**, 6503 (2011).

[12] M.I. Fedorov, E.A. Gurieva, I.S. Eremin, P.P. Konstantinov, A.Yu. Samunin,V.K. Zaitsev, S. Sano, L. Rauscher, Proceedings of the 2nd European conference on Thermoelectrics (AGH, Krakow, 2004), p. 72.

[13] V.K. Zaitsev, E.N. Tkalenko, E.N. Nikitin. Sov. Phys. Solid State, **11**, 221 (1969).

[14] G. Busch, U. Winkler. Helv. Phys. Acta, **26**, 578(1953).

[15] R.G. Morrison, R.D. Fedin, G.C. Danielson. Phys. Rev., **109**, 1909 (1958).

[16] E.N. Nikitin, V.G. Bazanov, V.I. Tarasov. Sov. Phys. Solid State, **3**, 2648 (1962).

[17] R.G. Morrison, R.D. Fedin, G.C. Danielson. Phys. Rev., **109**, 1916 (1958).

[18] M.W. Heller, G.C. Danielson. J. Phys. Chem. Solids., **23**, 601 (1962).

[19] J. Tani, H. Kido. Physica B, **364**, 218 (2005).

[20] H. Ihou-Mouko, C. Mercier, J. Tobola, G. Pont, H. Scherrer. J. Alloya and Compounds, **509**, 6503 (2011).

[21] L. Chuang, N. Savvides, T.T. Tan, S. Li. J. Chemistry and Material Science, **39**, 1971 (2010).

[22] J. Tani, H. Kido. Intermetalics, **15**, 1202 (2007).

[23] N.G. Galkin, K.N. Galkin, D.L. Goroshko, I.M. Chernev, A.V. Shevlyagin. JJAP, **54**, 07JC06, (2015)

[24] E. Kótai Nucl. Instrum. Methods. Phys. Rev. B **85**, 588, (1994)

[25] Z. Zolnai et al., Appl. Surf. Sci. **327**, 43 (2015)

[26] W.B. Whitten, P.L. Chung, and G.C. Danielson. J. Phys. Chem. Solids., **26**, 1753 (1965).

[27] D. McWilliams and D.W. Linch. Phys. Rev., **130**, 2248 (1963).

[28] T.I. Dyuzheva et al., Sov. Phys. Crystallogr. (Engl. Transl.) **17,** 705 (1973).

[29] Rohatgi et al. Sol. St. El. 23, 415 (1980)

[30] H. Lemke Phys. Stat. Sol. (a) 83,637 (1984)

[31] J. R. Troxel Solid. St. El. 26, 539 (1983)

Figure caption

Fig. 1 (a) RBS spectra measured by 1 MeV He^+ of the Al doped (red circle) and undoped (blue triangle) Mg_2Sn samples at 7° sample tilt angle. Surface edges for Sn, Mg, and Si are indicated by arrows. (b) RBS spectra of the undoped Mg_2Sn sample measured at 7° (black dot) and 60° (open dot) sample tilt, and with the fitted curves by the RBX program (7° blue line, 60° red line).

Fig.2 Average Raman spectra of the Al doped and undoped Mg_2Sn samples are shown by red line-dots and green line-triangles, respectively**.**

Fig. 3 Raman intensity maps of the undoped Mg_2Sn sample in the 200-235cm^{-1} (a) and in the 240-270 cm^{-1}(b) spectral range. The intensity maps of the two peaks show anticorrelation.

Fig.4 **a** Ratio of the Mg_2Sn and Mg_2Si Raman line intensities in the area shown in Fig.3. **b** Intensity map of the Si related Raman line. Some regions are covered by oxides transparent to the light used in Ranan measurement.

Fig. 5 HR XTEM pattern of the undoped Mg_2Sn sample. The framed area have marked characteristic of the periodic structure (1) and (2) in the film. FFT image of the HR XTEM pattern with reflections from periodic structures are shown in the insert.

Fig.6 XTEM image of the undoped Mg_2Sn sample. The layer is inhomogeneous and the thickness is in agreement with results of RBS model fit.

Fig. 7 Elementary maps in the undoped Mg_2Sn sample of the region shown in XTEM image in Fig.6. **a**: Mg map **b**: Sn map **c**: Si map **d**: O map.

Fig.8 HRTEM image of the undoped Mg_2Sn sample 1 year after the XTEM sample preparation.

Fig. 9 Elementary maps of the area degraded during 1 year storage in ambient shown in Fig.8 HRTEM image. **a:** Sn map **b:** O map **c:** Si map **d:** C map.

Fig. 10 The AFM height image of a 10x10 mm area of the uncovered Mg_2Sn sample about 18 month storage in ambient after the removing the samples from the vacuum chamber. The image proves that the change of the grown layer is so strong, that preparation a protective layer is vital in future study of these materials.

Fig.11 I-V characteristics of the Schottky junctions prepared over **a:** undoped Mg_2Sn layer; **b:** Al doped Mg_2Sn layer grown on p-type silicon measured at 77 K (blue) and 300 K (red).

Fig.12 Temperature dependence of the electrical characteristics of the Schottky junctions prepared over the Al doped and undoped Mg_2Sn layers grown on p-type silicon. **a** Capacitance **b** Current.

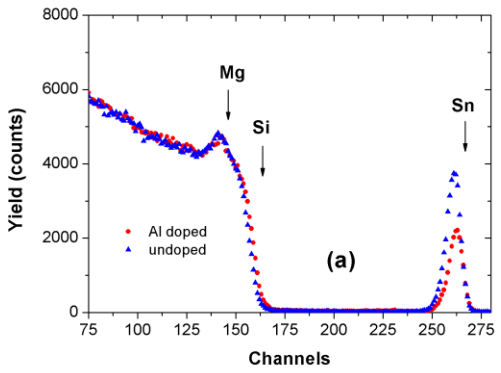

Fig. 1a

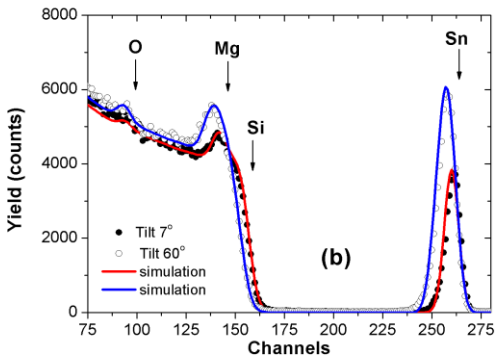

Fig.1b

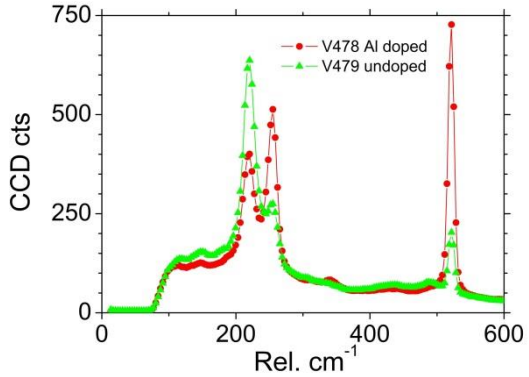

Fig.2

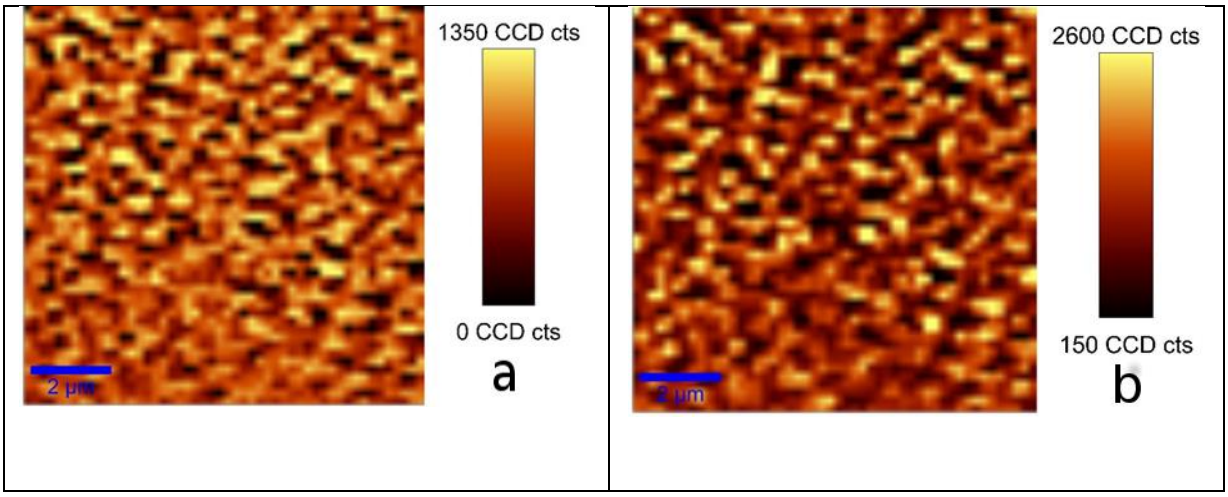
1350 CCD cts
0 CCD cts
a
2 µm
2600 CCD cts
150 CCD cts
b
2 µm

Fig. 3

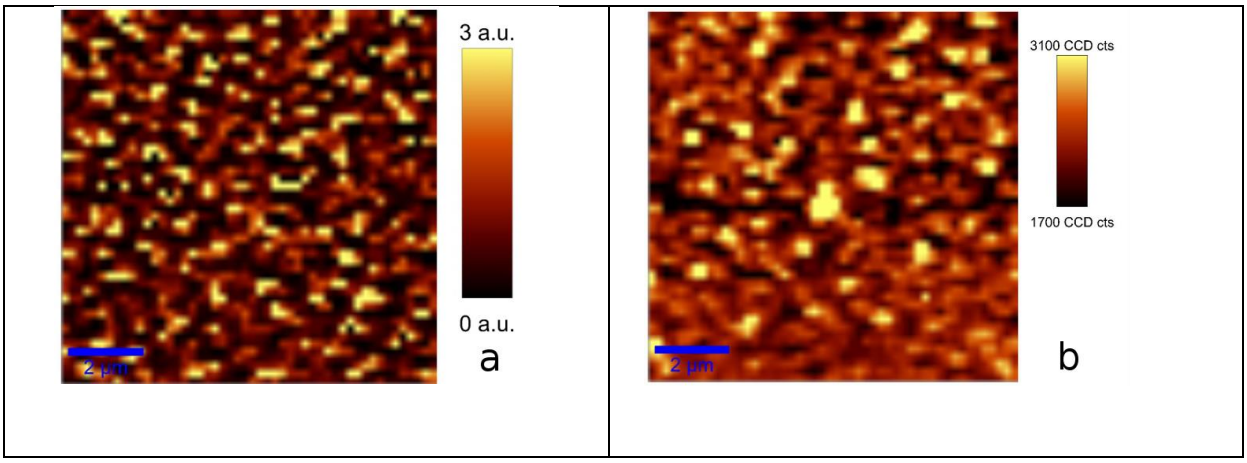
3 a.u.
0 a.u.
a
2 µm
3100 CCD cts
1700 CCD cts
b
2 µm

Fig. 4

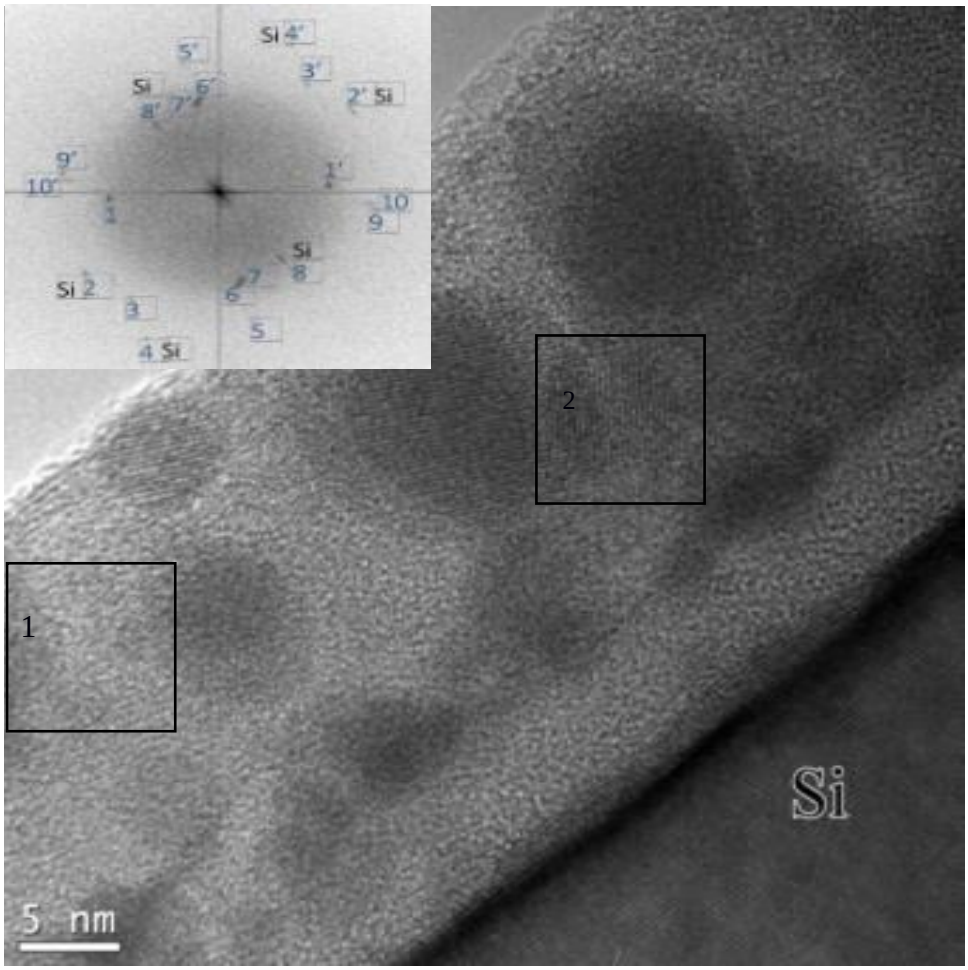

Fig. 5

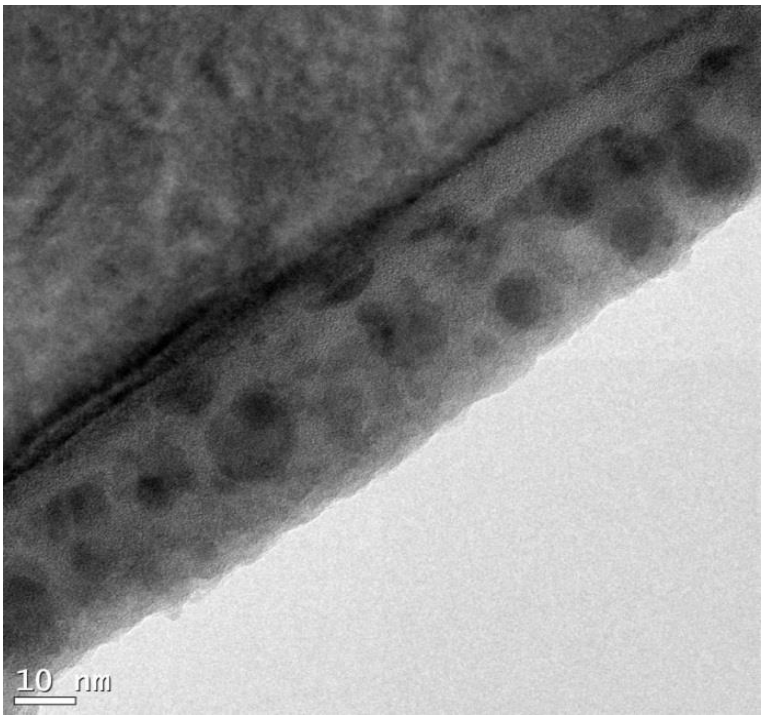

Fig.6

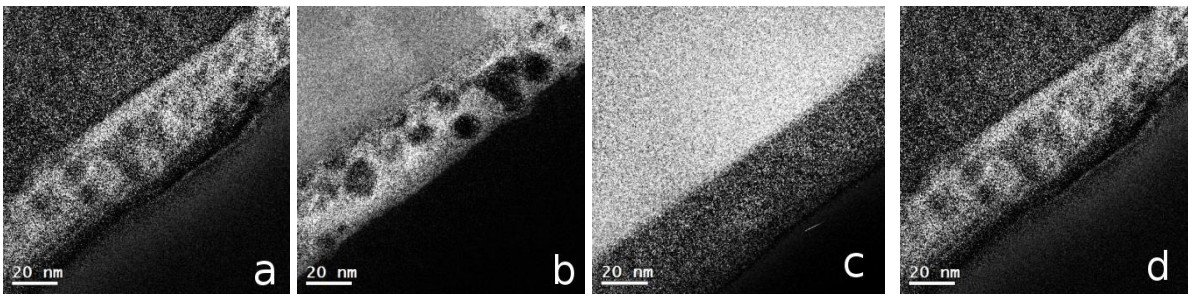

Fig. 7

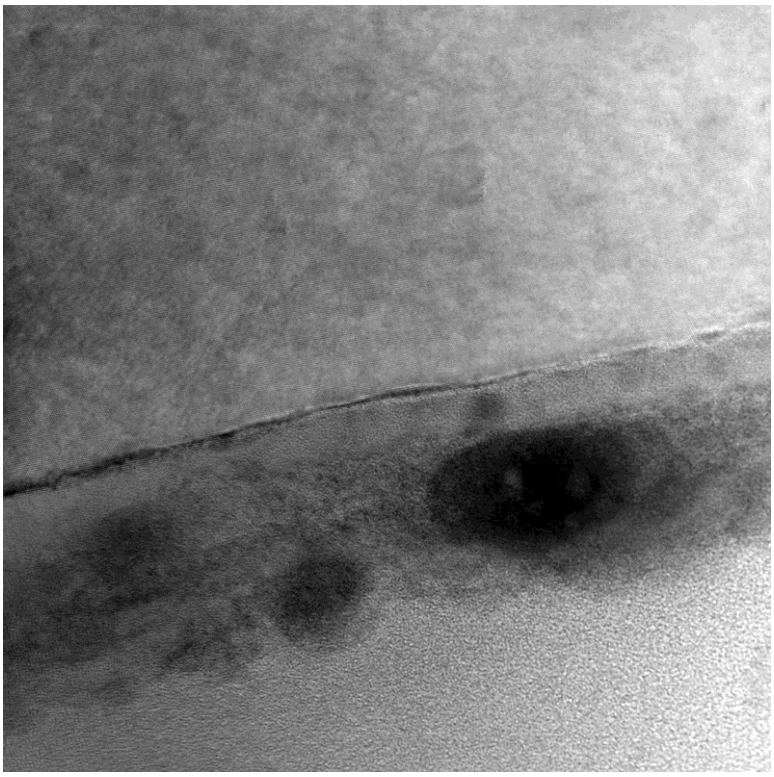

Fig.8

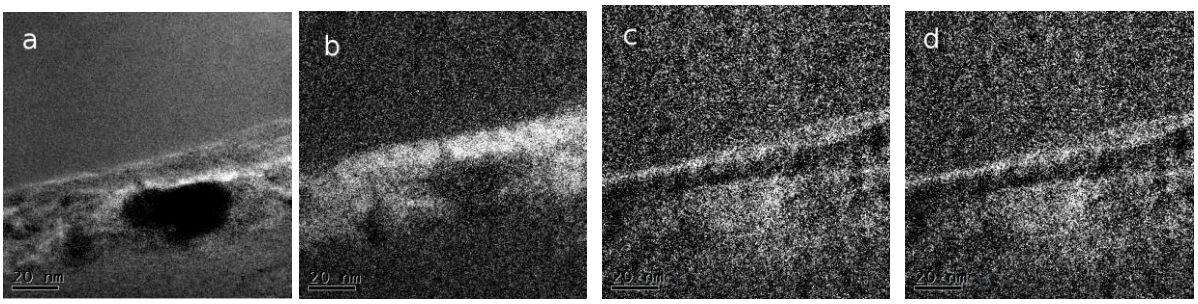

Fig. 9

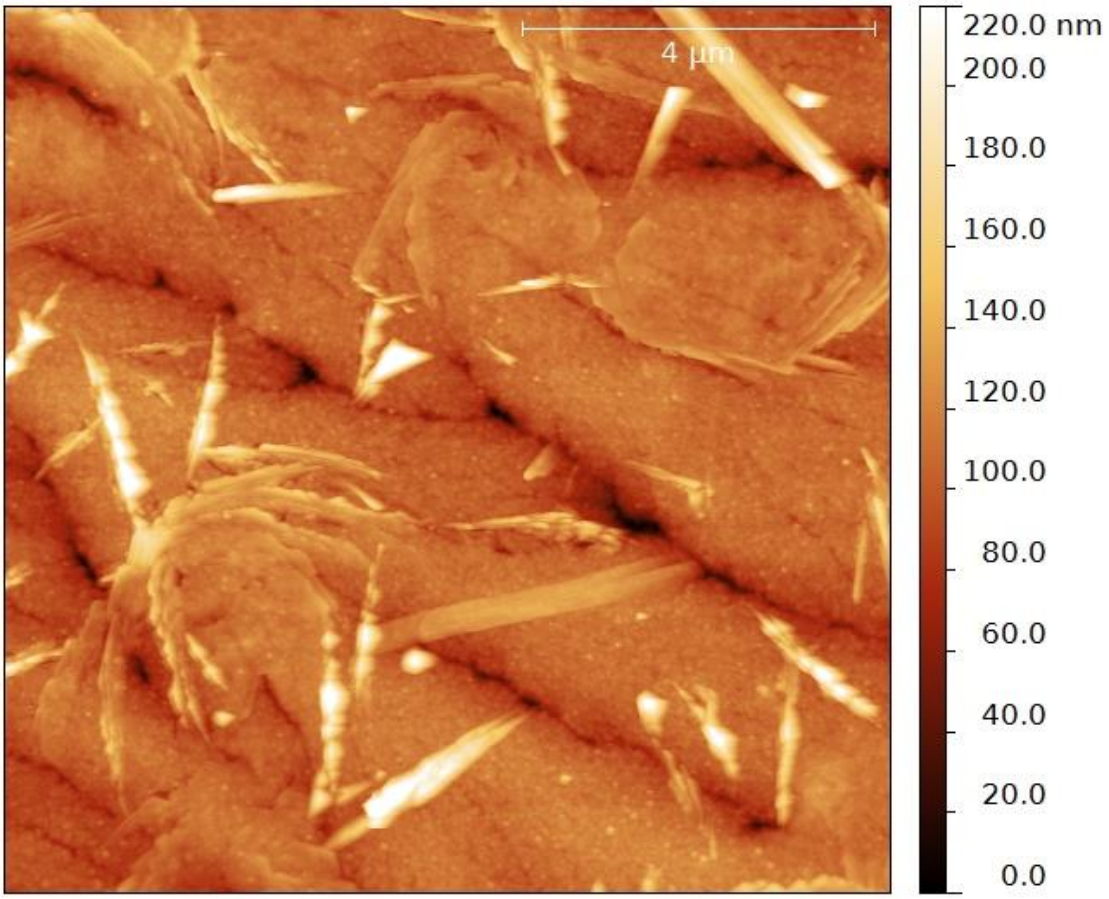

F*ig. 10*

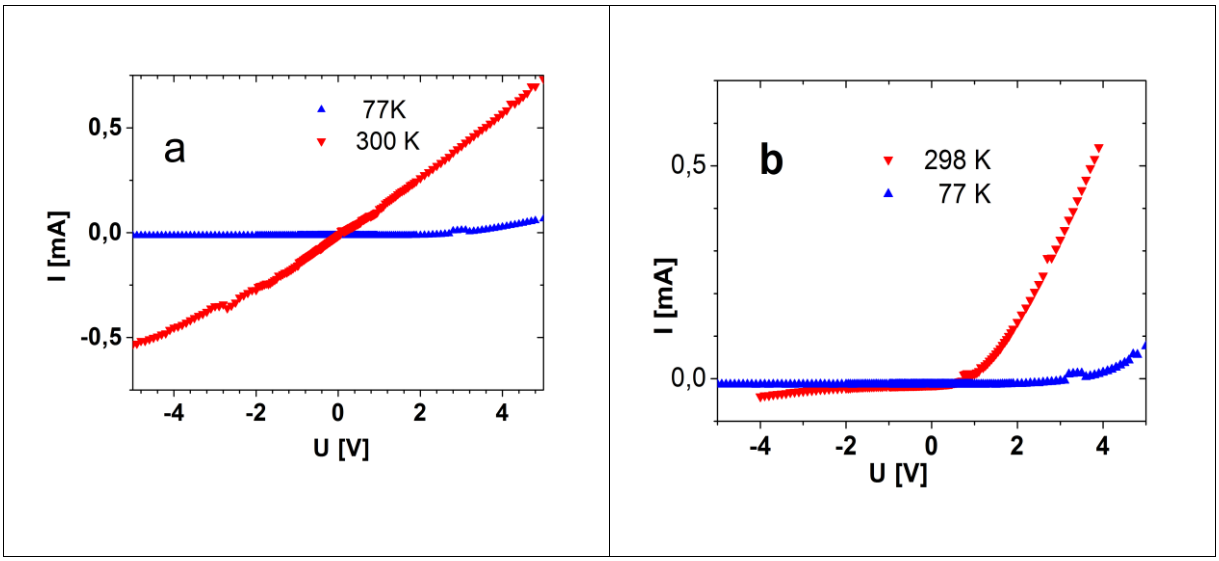
a
77K
300 K
I [mA]
U [V]
b
298 K
77 K
I [mA]
U [V]

Fig. 11

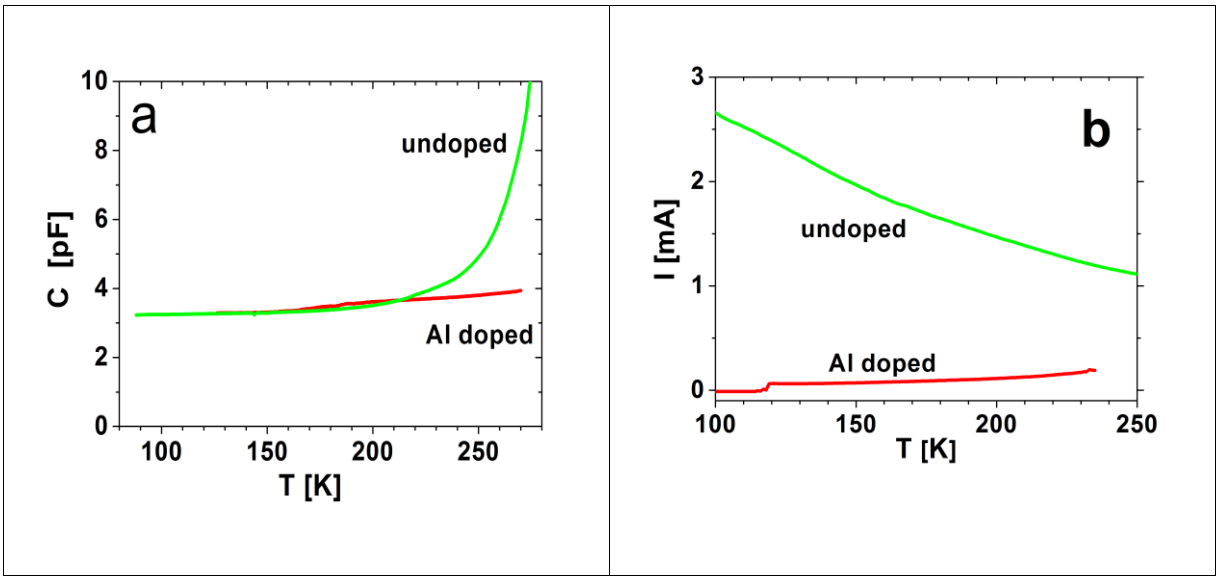
a
undoped
Al doped
C [pF]
T [K]
b
undoped
Al doped
I [mA]
T [K]

Table I. The deposited layers for Mg_2Sn formation on silicon. The layers were deposited 8 times, and annealed at 150 °C for 10 minutes after finishing the 8 deposition cycles.

	Al doped Mg_2Sn	Undoped Mg_2Sn
Sn	2.7 nm	2.7 nm
Al	0.13 nm	-
Mg	6.5 nm	6.5 nm

Table II. The thickness layer model and compositions of the Al doped Mg_2Sn sample calculated by fitting the RBS data using a two-layer model.

	Al doped Mg_2Sn	atom/cm^2
1st layer	$Sn_{0.125}Mg_{0.375}O_{0.5}$	5×10^{16}
2nd layer	$Sn_{0.06}Mg_{0.4}Si_{0.54}$	8×10^{16}

Table III. The thicknesses compositions of the undoped Mg_2Sn sample determined by fitting of the RBS data with a three-layer model.

	undoped Mg_2Sn	atom/cm^2
1st layer	$Sn_{0.1}Mg_{0.5}O_{0.4}$	7×10^{16}
2nd layer	$Sn_{0.25}Mg_{0.75}$	3×10^{16}
3rd layer	$Sn_{0.08}Mg_{0.5}Si_{0.42}$	7×10^{16}